



**HAL**  
open science

## Influence of Interference in MIMO Power Line Communication Systems

Thanh Nhân Vo, Karine Amis Cavalec, Thierry Chonavel, Pierre Siohan,  
Pascal Pagani

► **To cite this version:**

Thanh Nhân Vo, Karine Amis Cavalec, Thierry Chonavel, Pierre Siohan, Pascal Pagani. Influence of Interference in MIMO Power Line Communication Systems. ISPLC 2014: 18th IEEE International Symposium on Power Line Communications and its Applications, Mar 2014, Glasgow, United Kingdom. pp.255 - 260, 10.1109/ISPLC.2014.6812320 . hal-01009997

**HAL Id: hal-01009997**

**<https://hal.science/hal-01009997v1>**

Submitted on 19 Jun 2014

**HAL** is a multi-disciplinary open access archive for the deposit and dissemination of scientific research documents, whether they are published or not. The documents may come from teaching and research institutions in France or abroad, or from public or private research centers.

L'archive ouverte pluridisciplinaire **HAL**, est destinée au dépôt et à la diffusion de documents scientifiques de niveau recherche, publiés ou non, émanant des établissements d'enseignement et de recherche français ou étrangers, des laboratoires publics ou privés.

# Influence of Interference in MIMO Power Line Communication systems

Thanh Nhan VO<sup>1</sup>, Karine AMIS<sup>1</sup>, Thierry CHONAVEL<sup>1</sup>, Pierre SIOHAN<sup>2</sup>, Pascal PAGANI<sup>1</sup>  
 1: Telecom Bretagne / UMR CNRS 6285 Lab-STICC; 2: Orange R&D Labs

**Abstract**—For a few years, MIMO technique has been considered as the key to increase the data rate in the next generation of power line communications. The HomePlug AV2 and ITU-T G.9963 technologies exploit the MIMO scheme to increase both data rate and coverage. In this paper, an updated MIMO-PLC modeling is derived and the analytic formula of the interference is developed. Based on the interference analysis, the signal to interference plus noise ratio (SINR) is calculated and compared to the signal to noise ratio (SNR). Finally, the degradation of system performance in terms of capacity due to the interference is shown.

**Index Terms**—MIMO, Power Line Communication, Interference, Modeling, System performance.

## I. INTRODUCTION

In the past decades, the use of Power Line Communication systems for high rate indoor broadband communications has spread rapidly. No-new-wire makes the PLC economically attractive for the indoor LAN and can be complementary with the wireless technologies such as WLAN.

Recent studies proved that MIMO-PLC promises significantly higher performance when compared to today's SISO-PLC systems to enable applications such as high definition multimedia contents [1]. The MIMO-PLC is feasible since a protective earth (PE) wire is available in addition to phase (P) and neutral (N) wires. In MIMO techniques, we exploit the spatial diversity at the receiver (Rx) as well as at the transmitter (Tx) sides to improve two system features: throughput and coverage. Many contributions in the literature [2], [3] suggested that the PLC capacity is increased by a factor of around 2 when a MIMO technique is used.

Firstly, this paper proposes an updated MIMO-PLC channel modeling. In [5], the MIMO-PLC model relies on the multipath SISO-PLC channel modeling and the empirical correlation between the channels. This model is simple and describes the physical characteristics of a MIMO-PLC channel with high accuracy. However, Tonello *et al.* [6] recently proposed a new and more precise SISO-PLC model. It allows to generate SISO-PLC channels with statistics that are in higher agreement with experimental results. In our study, a MIMO-PLC channel modeling based on Hashmat's model [5] combined with the new SISO model of Tonello [6] is used.

Then, based on this modeling, an analytic expression of the interference and of the signal to interference plus noise ratio (SINR) taking into account the channel Tx and Rx filters parameters are derived. At the Rx side, the SINR determines the transmission quality, i.e. the error probability corresponding to a fixed data rate or the data rate at a fixed error probability.

Finally, the capacity degradation caused by the interference is shown. Those contributions will be interesting for further analysis and design of MIMO-PLC systems.

The paper is organized as follows. Section II details an improved model for MIMO-PLC channels. Section III details the analytic interference calculation for MIMO-PLC systems. In Section IV, we provide simulation results for SINR and capacity in MIMO-PLC systems. In particular, we study the impact of interference on system performance. Finally, some conclusions about the degradation of system performance due to interference are given in Section V.

## II. MIMO-PLC MODELING

We model the PLC channel response in the frequency domain. The European project OMEGA [7] defined a stochastic channel model based on an extensive sounding campaign and proposed nine classes corresponding to different severity levels. An analytical model was also proposed as an extension of Zimmermann's model [8] with a more accurate description of multipath. Tonello provided a statistical description of the model parameters in [9] and further developed this model in [6]. The frequency response of the SISO-PLC channel is

$$H(f) = A \sum_{n=1}^{N_p} (g_n + c_n f^{K_2}) e^{-(a_0 + a_1 f^K) l_n} e^{-j2\pi f l_n / \nu} \quad (1)$$

where  $\nu$  is the speed of electromagnetic waves in the copper medium,  $N_p$  is the number of propagation paths, and  $l_n$  is the length of the  $n$ -th path. Parameters  $A$  and  $g_n$  relate to the path amplitude, while parameters  $a_0$ ,  $a_1$ ,  $K$ ,  $K_2$  and  $c_n$  govern the frequency dependence of the channel transfer function. The values of the parameters for each of the nine classes can be found in [6].

In practice, a 2x4 MIMO scheme could be used for indoor PLC. At the transmitter, Kirchhoff's law limits the number of differential input ports to two among the three possibilities (P-N, P-PE and N-PE). At the receiver, MIMO processing of the three differential ports is beneficial. In addition, reception of the Common Mode (CM) signal can further improve the channel capacity. In [4], it is shown that in MIMO-PLC channels, a spatial correlation is inevitable and channels are not spatially independent. In [5], MIMO-PLC channels are modeled by taking into account the correlation between different channels. Firstly, the SISO-PLC channel, i.e. channel PN-PN (Tx P-N and Rx P-N) is initially generated by Tonello's model [9]. The other differential channels are obtained from the multipath used to generate the PN-PN channel by multiplying each path

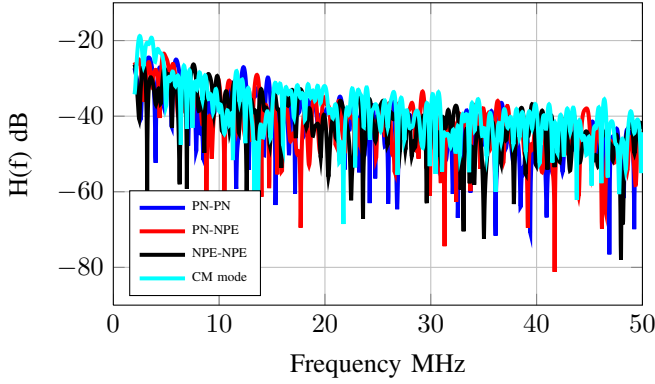


Fig. 1: Simulated MIMO-PLC class 2 channel.

with a fixed attenuation and adding a random phase shift to each of them. The resulting channel frequency response between the  $i$ -th Tx port and the  $k$ -th Rx port in [5] can be written as

$$H^{ki}(f) = A (\Delta A)^{ki} \sum_{n=1}^{N_p} g_n e^{-j\phi_n^{ki}} e^{-(a_0 + a_1 f^K)l_n} e^{-j2\pi f l_n / \nu} \quad (2)$$

where  $(\Delta A)^{ki}$  is an attenuation constant,  $\phi_n^{ki}$  is a random variable, uniformly distributed over  $[-(\Delta\Phi)^{ki}/2, (\Delta\Phi)^{ki}/2]$ . The values of  $(\Delta A)^{ki}$  and  $(\Delta\Phi)^{ki}/2$  are given in [5] on the basis of measurements involving differential MIMO channels. In this paper, we don't take into account the Common Mode.

To update existing MIMO-PLC channel models, we propose to combine Tonello's improved SISO-PLC channel model [6] and Hashmat's model [5] of MIMO-PLC channel. The SISO-PLC PN-PN channel is initially generated by (1) and the other MIMO channels are generated automatically, based on the generated PN-PN channel and Hashmat's model, that is, by adding random phase shift and fixed attenuation. The resulting channel frequency response between the  $i$ -th Tx port and the  $k$ -th Rx port can be written as

$$H^{ki}(f) = A (\Delta A)^{ki} \sum_{n=1}^{N_p} (g_n + c_n f^{K_2}) \times \left( e^{-j\phi_n^{ki}} e^{-(a_0 + a_1 f^K)l_n} e^{-j2\pi f l_n / \nu} \right) \quad (3)$$

Since the MIMO-PLC channel modeling is based on the nine classes of SISO-PLC channel in the Tonello's model, thus there are also nine classes for the MIMO-PLC channel in the updated model. Fig. 1 is an example of MIMO-PLC channel simulated with the updated model.

### III. INTERFERENCE ANALYSIS

For the sake of simplicity, we consider a 2x2 MIMO-PLC spatial multiplexing system. The demodulated sample at the Rx port  $k \in \{1, 2\}$  corresponding to the  $m_0$ -th subcarrier and  $n_0$ -th OFDM symbol denoted  $y^k(m_0, n_0)$  is

$$y^k(m_0, n_0) = \sum_{i=1}^2 y^{ki}(m_0, n_0) + n^k(m_0, n_0) \quad (4)$$

where  $y^{ki}(m_0, n_0)$  is the demodulated signal from Tx port  $i$  to Rx port  $k$  and  $n^k(m_0, n_0)$  is the noise sample on the  $m_0$ -th subcarrier and  $n_0$ -th OFDM symbol at the  $k$ -th Rx port.

In [10],  $y^{ki}(m_0, n_0)$  can be expressed as

$$y^{ki}(m_0, n_0) = \sum_{m=0}^{M-1} \sum_{n=-\infty}^{+\infty} s_{m,n}^i \sum_{l=0}^{P^{ki}-1} h_l^{ki} e^{-j2\pi m F_0 \tau_l^{ki}} \quad (5)$$

$$\times \underbrace{\frac{1}{T_0} \int_{-\infty}^{+\infty} g(t - nT - \tau_l^{ki}) f(t - n_0 T) e^{j2\pi(m-m_0)F_0 t} dt}_{I_g(m-m_0, n, n_0, \tau_l^{ki})}$$

where:

- $s_{m,n}^i$ : complex QAM, 8-PSK or BPSK symbol transmitted on the  $m$ -th subcarrier of the  $n$ -th OFDM symbol at Tx port  $i$ ;
- $M$ : total number of subcarriers;
- $T$ : OFDM symbol period;
- $GI, RI$ : Guard Interval, Roll-off Interval ( $GI > RI$ );
- $F_0, T_0 = T - GI = \frac{1}{F_0}$ : frequency between adjacent carriers, FFT window period;
- $g(t), f(t)$ : filter responses at Tx and Rx sides, respectively, specified in the IEEE P1901 standard [11]. The maximum amplitude of both  $g(t)$  and  $f(t)$  is 1.
- $h^{ki}(t) = \sum_{l=0}^{P^{ki}-1} h_l^{ki} \delta(t - \tau_l^{ki})$ : Multipath channel impulse response from the  $i$ -th Tx port to the  $k$ -th Rx port,  $h^{ki}(t) = \text{IFFT}(H^{ki}(f))$ ;

In (5), the term  $I_g(m - m_0, n, n_0, \tau_l^{ki})$  is the most complex one. In the following, we derive  $I_g(m - m_0, n, n_0, \tau_l^{ki})$  depending on the  $\tau_l^{ki}$  value. Figures 2 and 3 show the relative position between filter responses at the Tx and at the Rx calculation of  $I_g(m - m_0, n, n_0, \tau_l^{ki})$  is given in Appendix A and is summarized below:

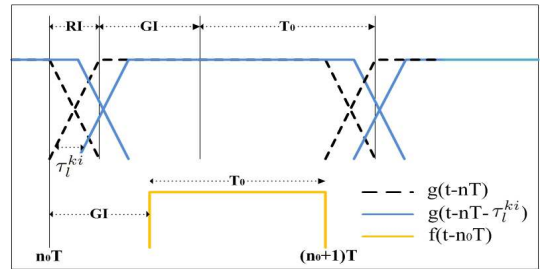


Fig. 2: Relative position between  $g(t - nT - \tau_l^{ki})$  and  $f(t - n_0 T)$  if  $\tau_l^{ki} < GI - RI$ .

- $\tau_l^{ki} < GI - RI$ :  

$$I_g(m - m_0, n, n_0, \tau_l^{ki}) = \delta(n - n_0) \delta(m - m_0) \quad (6)$$
- $GI - RI < \tau_l^{ki} < T$ : Based on the illustration in Fig. 3, the term  $I_g(m - m_0, n, n_0, \tau_l^{ki})$  is not null if and only if  $n = n_0$  or  $n = n_0 - 1$ .

**If  $n = n_0$ , we obtain:**

$$I_g(m - m_0, n, n_0, \tau_l^{ki}) = V(m - m_0, n_0) \delta(m - m_0) - A_g(m - m_0, n_0, \tau_l^{ki}) \quad (7)$$

where  $V(m - m_0, n_0)$  and  $A_g(m - m_0, n_0, \tau_l^{ki})$  are given in Appendix A.

**If  $n = n_0 - 1$ , with the same calculation and taking into account  $g(u + T) = 1 - g(u)$ ,  $\forall u \in [0, RI]$  we obtain:**

$$I_g(m - m_0, n, n_0, \tau_l^{ki}) = A_g(m - m_0, n_0, \tau_l^{ki}) \quad (8)$$

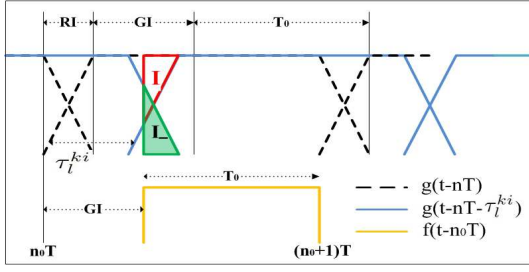


Fig. 3: Relative position between  $g(t - nT - \tau_l^{ki})$  and  $f(t - n_0T)$  if  $GI - RI < \tau_l^{ki} < T$ .

The channel response  $h^{ki}(t) = \sum_{l=0}^{P^{ki}-1} h_l^{ki} \delta(t - \tau_l^{ki})$  where  $\tau_l^{ki} < \tau_{l+1}^{ki}$  and  $\tau_{L^{ki}-1}^{ki} < GI - RI < \tau_{L^{ki}}^{ki}$  can be rewritten as

$$h^{ki}(t) = \sum_{l=0}^{L^{ki}-1} h_l^{ki} \delta(t - \tau_l^{ki}) + \sum_{l=L^{ki}}^{P^{ki}-1} h_l^{ki} \delta(t - \tau_l^{ki}) \quad (9)$$

Replacing (9) into (5) and taking into account (6), (7) and (8), the analytic formula of  $y^{ki}(m_0, n_0)$  is derived as

$$\begin{aligned} & \sum_{m=0}^{M-1} \sum_{n=-\infty}^{+\infty} s_{m,n}^i \sum_{l=0}^{L^{ki}-1} h_l^{ki} e^{-j2\pi m F_0 \tau_l^{ki}} \delta(n - n_0) \delta(m - m_0) \\ & + \sum_{m=0}^{M-1} \sum_{n=-\infty}^{+\infty} s_{m,n}^i \sum_{l=L^{ki}}^{P^{ki}-1} h_l^{ki} e^{-j2\pi m F_0 \tau_l^{ki}} \{\delta(n - n_0) [\delta(m - m_0) \\ & - A_g(m - m_0, n, \tau_l^{ki})] + \delta(n - n_0 + 1) A_g(m - m_0, n_0, \tau_l^{ki})\} \\ & = s_{m_0, n_0}^i \sum_{l=0}^{P^{ki}-1} h_l^{ki} e^{-j2\pi m_0 F_0 \tau_l^{ki}} + \sum_{m=0}^{M-1} (s_{m, n_0-1}^i - s_{m, n_0}^i) \\ & \quad \times \sum_{l=L^{ki}}^{P^{ki}-1} h_l^{ki} e^{-j2\pi m F_0 \tau_l^{ki}} A_g(m - m_0, n_0, \tau_l^{ki}) \\ & = s_{m_0, n_0}^i \underbrace{(H^{ki}(m_0 F_0) - \sum_{l=L^{ki}}^{P^{ki}-1} h_l^{ki} e^{-j2\pi m_0 F_0 \tau_l^{ki}} A_g(0, n_0, \tau_l^{ki}))}_{\alpha^{ki}(m_0)} \\ & - \underbrace{\sum_{m=0, m \neq m_0}^{M-1} s_{m, n_0}^i \sum_{l=L^{ki}}^{P^{ki}-1} h_l^{ki} e^{-j2\pi m F_0 \tau_l^{ki}} A_g(m - m_0, n_0, \tau_l^{ki})}_{I^{ki}(m_0, n_0)} \\ & + \underbrace{\sum_{m=0}^{M-1} s_{m, n_0-1}^i \sum_{l=L^{ki}}^{P^{ki}-1} h_l^{ki} e^{-j2\pi m F_0 \tau_l^{ki}} A_g(m - m_0, n_0, \tau_l^{ki})}_{I^{ki}(m_0, n_0-1)} \end{aligned} \quad (10)$$

The terms  $I^{ki}(m_0, n_0)$  and  $I^{ki}(m_0, n_0 - 1)$  are the interference from the  $n_0$ -th and  $(n_0 - 1)$ -th OFDM symbol to the  $m_0$ -th subcarrier on the  $n_0$ -th OFDM symbol. They are caused by the paths whose delay is greater than  $GI - RI$ .

$$I^{ki}(m_0, n_0) = \sum_{\substack{m=0 \\ m \neq m_0}}^{M-1} s_{m, n_0}^i V(m - m_0, n_0) \mathcal{W}_{ki}(m, m_0) \quad (11)$$

where  $\mathcal{W}_{ki}(m, m_0) = \sum_{l=L^{ki}}^{P^{ki}-1} h_l^{ki} e^{-j2\pi m F_0 \tau_l^{ki}} \frac{1}{T_0} \int_{GI}^{\tau_l^{ki} + RI} (1 - g(u - \tau_l^{ki})) e^{j2\pi(m - m_0) F_0 u} du$ .

We assume that the  $s_{m,n}^i$  are independently and identically distributed  $\forall i, m, n$  with zero mean and variance  $\sigma_s^2(m, n, i)$ . The power contributions of  $I^{ki}(m_0, n_0)$  and of  $I^{ki}(m_0, n_0 - 1)$  are written as

$$\mathcal{P}_1 = E[|I^{ki}(m_0, n_0)|^2] = \sum_{\substack{m=0 \\ m \neq m_0}}^{M-1} \sigma_s^2(m, n_0, i) |\mathcal{W}_{ki}(m, m_0)|^2$$

$$\mathcal{P}_2 = E[|I^{ki}(m_0, n_0 - 1)|^2] = \sum_{m=0}^{M-1} \sigma_s^2(m, n_0 - 1, i) |\mathcal{W}_{ki}(m, m_0)|^2$$

We assume that the channel is time-invariant and the power allocation  $P_i(m) = \sigma_s^2(m, n, i)$ ,  $\forall n$ . Then, the total interference power is rewritten as

$$\mathcal{P}_I^{ki}(m_0, n_0) = \mathcal{P}_1 + \mathcal{P}_2 = \sum_{m=0}^{M-1} P_i(m) \Gamma^{ki}(m, m_0) \quad (12)$$

where  $\Gamma^{ki}(m, m_0) = 2|\mathcal{W}_{ki}(m, m_0)|^2$  if  $m \neq m_0$  and  $\Gamma^{ki}(m_0, m_0) = |\mathcal{W}_{ki}(m_0, m_0)|^2$ .

Taking into account Eq. (10) and under the assumption of time-invariant channels, we can rewrite (4) under the matrix form as

$$\mathbf{Y}_{m_0} = \mathbf{A}_{m_0} \mathbf{S}_{m_0} + \mathbf{I}_{m_0} + \mathbf{N}_{m_0}, \quad (13)$$

where  $\mathbf{Y}_{m_0} = [y^k(m_0)]^T$ ;  $k = 1, 2$ ;

$$\mathbf{A}_{m_0} = \begin{bmatrix} \alpha^{11}(m_0) & \alpha^{12}(m_0) \\ \alpha^{21}(m_0) & \alpha^{22}(m_0) \end{bmatrix}; \mathbf{S}_{m_0} = [s_{m_0}^1 \quad s_{m_0}^2]^T$$

$$\mathbf{I}_{m_0} = [\sum_i (I^{ki}(m_0) + I_{-}^{ki}(m_0))]^T \\ = [I_1(m_0), I_2(m_0)]^T;$$

where  $I^{ki}(m_0)$  (resp.  $I_{-}^{ki}(m_0)$ ) is the interference contribution of the current (resp. the previous) OFDM symbol to the  $m_0$ -th subcarrier.

$$\mathbf{N}_{m_0} = [n^k(m_0)]^T.$$

The covariance matrix of the noise plus interference is

$$\mathbf{X}_{IN}(m_0) = E[(\mathbf{I}_{m_0} + \mathbf{N}_{m_0})(\mathbf{I}_{m_0} + \mathbf{N}_{m_0})^H] \quad (14)$$

It can be rewritten as

$$\mathbf{X}_{IN}(m_0) = \begin{bmatrix} E[I_1 I_1^*](m_0) + \sigma_1^2(m_0) & E[I_1 I_2^*](m_0) \\ E[I_2 I_1^*](m_0) & E[I_2 I_2^*](m_0) + \sigma_2^2(m_0) \end{bmatrix} \quad (15)$$

Indeed, the covariance matrix  $\mathbf{X}_{IN}(m_0)$  depends on the power allocated at all transmitters and on all used subcarriers because the terms  $E[I_a I_b^*](m_0)$  (after some algebra) depend on the power allocation  $P_1(m)$ ,  $P_2(m)$ ,  $\forall m$  (see Appendix B).

Since the number of used subcarriers employed in practical PLC systems is quite large, we assume that the interference on a given subcarrier is normally distributed (following the central limit theorem). Different normality tests for the interference have been introduced in [12]. It shows that our assumption is valid in practical PLC systems. Under a gaussian continuous input distribution, taking into account the interference and assuming that a channel knowledge is available at the receiver, the theoretical capacity is given by [13]

$$\begin{aligned} & C_{MIMO}(m_0) \\ & = \log_2 \left( \det(\mathbf{I}_{2 \times 2} + \mathbf{X}_{IN}^{-1}(m_0) \mathbf{A}(m_0) \mathbf{Q}(m_0) \mathbf{A}^H(m_0)) \right) \end{aligned} \quad (16)$$

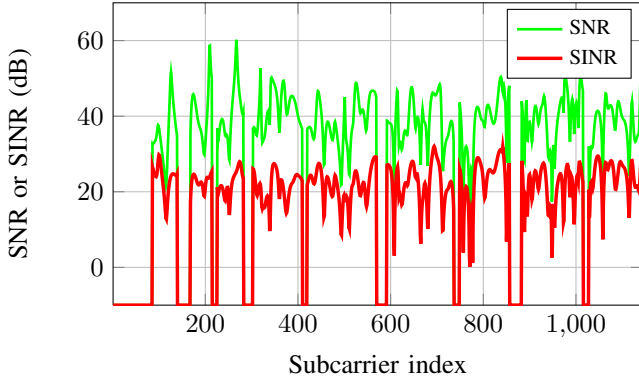


Fig. 4: SINR and SNR comparison at the P-N receiver port (MIMO-PLC class 2 channel).

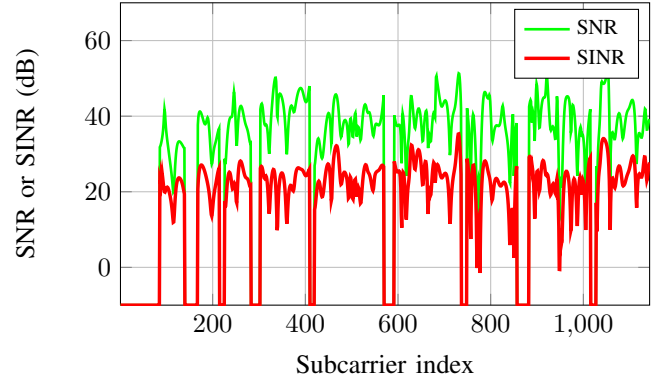


Fig. 5: SINR and SNR comparison at the N-PE receiver port (MIMO-PLC class 2 channel).

where  $\mathbf{Q}(m_0) = \text{diag}([P_1(m_0) \ P_2(m_0)])$ .

When the interference in (13) is neglected, the theoretical capacity can be approximated by [1], [2]:

$$\hat{C}_{MIMO}(m_0) = \sum_{i=1}^2 \log_2 \left( 1 + \frac{\lambda_i(m_0)P_i(m_0)}{\sigma_i^2(m_0)} \right) \quad (17)$$

where  $\lambda_i(m_0)$  is the  $i$ -th eigenvalue of  $\mathbf{A}(m_0)\mathbf{A}^H(m_0)$ .

In the simulation part, we compare the theoretical capacity given by (16) with its approximation (17) and then we discuss the influence of interference into MIMO-PLC systems in terms of capacity.

#### IV. SIMULATION RESULTS

The simulation parameters are fixed by the IEEE P1901 standard [11]:

- Number of used subcarriers  $L = 917$  corresponding to the used frequency band 2-28 MHz.
- $f_s = 100$  MHz,  $F_0 = \frac{1}{T_0} = 24.414$  kHz,  $GI = 5.56$   $\mu$ s,  $RI = 4.96$   $\mu$ s,  $T = 46.52$   $\mu$ s,  $M = 4096$ .
- Channel model  $H^{ki}(f)$ : SISO-PLC Class 2 channel of Tonello's model [6] and 2x2 MIMO-PLC (same circuit using P-N, N-PE) of Hashmat's model [5].
- The channel impulse response  $h^{ki}(t)$  is derived from  $H^{ki}(f)$  by applying IFFT and time rectangular filtering, keeping 95% of the initial energy [7].
- Noise model: the noise vector has independent colored gaussian components simulated with the extension of Esmailian's model [14].
- Spectral mask constraint:  $P_1(m) + P_2(m) \leq P_0$ ,  $\forall m$ . The total power allocated on any subcarrier is less than or equal  $P_0$ , where  $P_0 = -55$  dBm/Hz [11].

We use the channel class 2 in the simulations as it modelizes the most frequent practical channel [7]. To illustrate the impact of interference, we use the minimum value of  $GI$  defined in the IEEE P1901, i.e.  $GI = 5.56$   $\mu$ s. The transmission quality depends both on noise and interference levels and we shall study the impact of interference when added to noise. We assume a Zero-Forcing (ZF) equalization on each subcarrier. At the ZF equalizer output, the interference plus noise level at the  $m_0$ -th used subcarrier on Rx port  $k$  is derived as follows:

$$P_{IN}^k(m_0) = \{\mathbf{w}_{m_0}\mathbf{X}_{IN}^{-1}(m_0)\mathbf{w}_{m_0}^H\}(k, k) \quad (18)$$

where  $\mathbf{w}_{m_0} = (\mathbf{A}^H(m_0)\mathbf{A}(m_0))^{-1}\mathbf{A}^H(m_0)$  is the coefficient matrix of the ZF equalizer at the  $m_0$ -th used subcarrier. The SINR at the  $k$ -th receiver on the  $m_0$ -th used subcarrier is

$$SINR^k(m_0) = \frac{P_k(m_0)}{P_{IN}^k(m_0)} \quad (19)$$

where  $P_k(m_0)$  is the power allocated at the  $k$ -th Tx port on the  $m_0$ -th used subcarrier. Note that the SNR can be also determined by replacing  $\mathbf{X}_{IN}(m_0)$  in (18) and (19) with  $\mathbf{X}_N(m_0) = \text{diag}([\sigma_1^2(m_0), \sigma_2^2(m_0)])$ .

Fig. 4 and (resp. Fig. 5) shows the SINR and SNR at the ZF equalizer output for the receiver port P-N (resp. N-PE) in the MIMO-PLC class 2 with the equal maximum power allocation,  $P_1(m) = P_2(m) = P_0/2$ ,  $\forall m$ . In these figures, the notches represent the unused subcarriers. The SNR level is always much higher than the SINR level on all subcarriers. The mean shift between SNR and SINR is about 17 dB at the P-N receiver and about 15 dB at the N-PE receiver. This demonstrates that the interference cannot be neglected and that it significantly degrades the transmission quality in the case of  $GI = 5.56$   $\mu$ s. In practice, the IEEE P1901 standard has also defined other longer guard interval (7.56  $\mu$ s and 47.12  $\mu$ s). The length of guard interval is negotiated after the channel estimation. The longer guard interval is chosen, the less impact of interference is, but the throughput may be also decreased.

To illustrate the capacity degradation due to interference, we compute the theoretical capacity given by (16) and its approximation (interference neglected). Table 1 shows the simulation results averaged over 200 channel realizations.

Total capacity (Mbits)	$P_1=P_2=P_0/2$	$P_1=P_2=P_0/32$
Exact (16)	373.8	356
Approximation (17)	706.4	527.8

Table 1. Theoretical capacity comparison in MIMO-PLC Class 2 channel.

In Eq. (16), the theoretical capacity  $C_{MIMO}$  depends on the power allocation at all subcarriers in a complex way. Thus, to evaluate the dependence of theoretical capacity on the power allocation, we also calculate the total theoretical capacity with equal power allocation  $P_1(m) = P_2(m) = P_0/32$ ,  $\forall m$ .

Simulation results are also given in Table 1. We can see that the exact capacity is much smaller than its approximation. Moreover, when the power allocation at every Tx port on every subcarrier changes from  $P_0/2$  to  $P_0/32$ , the value given by the approximation is significantly reduced. However, this is not the case for the value obtained with the exact formulation because not only  $\mathbf{Q}(m_0)$  but also  $\mathbf{X}_{IN}(m_0)$  depend on the power allocation. The capacity shift in the former case (latter case) is about 25% (5%). Thus, while the equal maximum power allocation with  $P_1(m) = P_2(m) = P_0/2$  is a simple and efficient strategy for conventional MIMO-OFDM systems without channel state information at Tx (CSIT) and under the assumption that interference is negligible, it should not be exploited in MIMO-PLC systems where interference cannot be neglected. In the presence of interference, even when the power allocation is multiplied by a factor of 16, the capacity keeps roughly the same. This can be explained by the fact that with the equal power allocation, the covariance matrix  $\mathbf{X}_{IN}(m_0)$  can be considered as  $\mathbf{X}_{IN}(m_0) = P \mathbf{W}(m_0)$  (see Appendix B), where  $P$  is the (scalar) power value allocated on every Tx port and on every subcarrier, i.e.  $P_1(m) = P_2(m) = P$  and  $\mathbf{W}(m_0)$  is a 2x2 matrix that can be considered independent from  $P$ . In this case, we obtain:

$$\begin{aligned} C_{MIMO}(m_0) & \quad (20) \\ &= \log_2 \left( \det \left( \mathbf{I}_{2 \times 2} + \mathbf{X}_{IN}^{-1}(m_0) \mathbf{A}(m_0) \mathbf{Q}(m_0) \mathbf{A}(m_0) \right) \right) \\ &= \log_2 \left( \det \left( \mathbf{I}_{2 \times 2} + (P\mathbf{W})^{-1}(m_0) \mathbf{A}(m_0) P \mathbf{I}_{2 \times 2} \mathbf{A}(m_0) \right) \right) \\ &= \log_2 \left( \det \left( \mathbf{I}_{2 \times 2} + \mathbf{W}^{-1}(m_0) \mathbf{A}(m_0) \mathbf{A}(m_0) \right) \right) \end{aligned}$$

The capacity doesn't depend on  $P$  if  $\mathbf{W}(m_0)$  is considered independent from  $P$ . However, this is valid for high SNR values only. Thus, there is a small capacity shift when  $P$  varies from  $P_0/2$  to  $P_0/32$ .

Simulations for MIMO-PLC Class 9 channel (SISO-PLC Class 9 channel of Tonello's model + 2x2 MIMO-PLC) are also shown and support the preceding comment. As the maximum delay spread of Class 9 channel is less than  $0.6 \mu\text{s}$  ( $= GI - RI$ ) in most of realizations, there is no interference or the interference is insignificant. Then, the exact capacity coincides with its approximation. Table 2 illustrates the simulation results for Class 9 channel.

Total capacity (Mbits)	$P_1=P_2=P_0/2$	$P_1=P_2=P_0/32$
Exact (16)	1232.9	1053.8
Approximation (17)	1232.9	1053.8

Table 2. Theoretical capacity comparison in MIMO-PLC Class 9 channel.

The simulation results in Tables 1 and 2 demonstrate that the interference can have a strong impact depending on the severity of the channel and must be considered in the optimization of PLC systems. In that case, equal power allocation is not an efficient solution and hence joint bit-loading/power allocation should be done. In practical systems, where the receiver cannot make the difference between noise and interference, the exact formula should be used.

## V. CONCLUSION

This paper has presented a detailed analysis of the MIMO-PLC interference and of the Signal to Interference plus Noise Ratio. It takes into account the channel characteristics and filter responses at the Tx and at the Rx sides. In this study, we have used the filters specified in IEEE P1901 standard to simulate the SINR in MIMO-PLC. The simulation results show that the SINR at both receiver ports is significantly less than the SNR in the case of class 2 channel when a  $GI$  of  $5.56 \mu\text{s}$  is used. Moreover, the degradation of transmission quality in terms of capacity is also carried out. It is also demonstrated that the equal maximum power allocation, i.e.  $P_1(m) = P_2(m) = P_0/2$ , which is used in conventional MIMO-OFDM systems with the assumption of no interference and no CSIT, is not a good strategy for the power allocation in such PLC channels and such length of guard interval. Future work will use this interference analysis to study bit/power allocation problem and propose an efficient strategy to solve it.

### APPENDIX A: CALCULATION OF $I_g(m - m_0, n, n_0, \tau_l^{ki})$

In this section, the analytic formula of  $I_g(m - m_0, n, n_0, \tau_l^{ki})$  is shown, depending on the value of  $\tau_l^{ki}$ .

- $\tau_l^{ki} < GI - RI$ : By observing Fig. 2, we obtain:

$$\begin{aligned} I_g(m - m_0, n, n_0, \tau_l^{ki}) &= \frac{1}{T_0} \int_{-\infty}^{+\infty} g(t - nT - \tau_l^{ki}) f(t - n_0T) e^{j2\pi(m - m_0)F_0 t} dt \\ &= \frac{1}{T_0} \delta(n - n_0) \int_{GI}^{GI+T_0} \underbrace{g(u - \tau_l^{ki})}_{=1} \underbrace{f(u)}_{=1} e^{j2\pi(m - m_0)F_0(u + n_0T)} du \\ &= e^{j2\pi(m - m_0)F_0(n_0T + GI)} \delta(n - n_0) \frac{1}{T_0} \int_0^{T_0} e^{j2\pi(m - m_0)F_0 w} dw \\ &= e^{j2\pi(m - m_0)F_0(n_0T + GI)} \delta(n - n_0) \delta(m - m_0) \\ &= \delta(n - n_0) \delta(m - m_0) \quad (21) \end{aligned}$$

where we use that  $T_0 = \frac{1}{F_0}$ ,  $u = t - n_0T$  and  $w = u - GI$ .

- $GI - RI < \tau_l^{ki} < T$ :

If  $\mathbf{n} = \mathbf{n}_0$ :

$$\begin{aligned} I_g(m - m_0, n, n_0, \tau_l^{ki}) &= \frac{1}{T_0} \int_{GI}^T g(u - \tau_l^{ki}) f(u) e^{j2\pi(m - m_0)F_0(u + n_0T)} du \\ &= \underbrace{e^{j2\pi(m - m_0)F_0 n_0 T}}_{V(m - m_0, n_0)} \frac{1}{T_0} \int_{GI}^T g(u - \tau_l^{ki}) e^{j2\pi(m - m_0)F_0 u} du \\ &= V(m - m_0, n_0) \left( \frac{1}{T_0} \int_{GI}^T e^{j2\pi(m - m_0)F_0 u} du \right. \\ &\quad \left. + \underbrace{\int_{GI}^{\tau_l^{ki} + RI} (g(u - \tau_l^{ki}) - 1) e^{j2\pi(m - m_0)F_0 u} du}_{-G(m - m_0, \tau_l^{ki})} \right) \\ &= V(m - m_0, n_0) \delta(m - m_0) - A_g(m - m_0, n_0, \tau_l^{ki}) \quad (22) \end{aligned}$$

where  $A_g(m - m_0, n_0, \tau_l^{ki}) = V(m - m_0, n_0)G(m - m_0, \tau_l^{ki})$ .

If  $\mathbf{n} = \mathbf{n}_0 - 1$ :

$$\begin{aligned} I_g(m - m_0, n, n_0, \tau_l^{ki}) &= \frac{1}{T_0} V(m - m_0, n_0) \int_{GI}^{\tau_l^{ki} + RI} g(u + T - \tau_l^{ki}) \\ &\quad \times e^{j2\pi(m - m_0)F_0 u} du \\ &= \frac{1}{T_0} V(m - m_0, n_0) \int_{GI}^{\tau_l^{ki} + RI} (1 - g(u - \tau_l^{ki})) \\ &\quad \times e^{j2\pi(m - m_0)F_0 u} du \\ &= A_g(m - m_0, n_0, \tau_l^{ki}) \end{aligned} \quad (23)$$

#### APPENDIX B: CALCULATION OF $\mathbf{X}_{IN}$

In this section, we demonstrate that  $E[I_a I_b^*](m_0)$  depends on the power allocation  $P_1(m)$ ,  $P_2(m)$ ,  $\forall m$ . To this end, we reuse Eq. (11) with the assumption of time invariant channel.

$$I^{ki}(m_0) = \sum_{m=0, m \neq m_0}^{M-1} s_m^i V(m - m_0) \mathcal{W}_{ki}(m, m_0) \quad (24)$$

$$I_-^{ki}(m_0) = \sum_{m=0}^{M-1} \hat{s}_m^i V(m - m_0) \mathcal{W}_{ki}(m, m_0) \quad (25)$$

where  $s_m^i$  and  $\hat{s}_m^i$  are the symbol allocated on the  $m$ -th subcarrier at the current OFDM symbol and the previous OFDM symbol (at Tx  $i$ ), respectively. Note that  $\{s_m^i\}$  and  $\{\hat{s}_m^i\}$  are mutually independent. Moreover,  $\{s_m^i\}$  (respectively  $\{\hat{s}_m^i\}$ ) is a sequence of independent and identically distributed symbols with zero mean. We can thus write:

$$E[s_m^i (\hat{s}_{m'}^i)^*] = 0 \quad \forall i, i', m, m'; \quad (26)$$

$$E[\hat{s}_m^i (\hat{s}_{m'}^i)^*] = E[s_m^i (\hat{s}_{m'}^i)^*] = 0 \quad \forall i \neq i', m, m'; \quad (27)$$

$$E[|s_m^i|^2] = E[|\hat{s}_m^i|^2] = P_i(m). \quad (28)$$

With Eq. (26), (27) and (28) we can obtain:

$$\begin{aligned} E[I^{ki}(m_0) (I^{k'i'}(m_0))^*] &= E[I^{ki}(m_0) (I_-^{k'i'}(m_0))^*] \\ &= \begin{cases} 0 & i \neq i' \\ \sum_{\substack{m=0 \\ m \neq m_0}}^{M-1} P_i(m) \mathcal{W}_{ki}(m, m_0) \mathcal{W}_{k'i}^*(m, m_0) & i = i' \end{cases} \end{aligned} \quad (29)$$

$$\begin{aligned} E[I_-^{ki}(m_0) (I_-^{k'i'}(m_0))^*] &= \begin{cases} 0 & i \neq i' \\ \sum_{m=0}^{M-1} P_i(m) \mathcal{W}_{ki}(m, m_0) \mathcal{W}_{k'i}^*(m, m_0) & i = i' \end{cases} \end{aligned} \quad (30)$$

Using (29), (30) and the definition of  $I_1(m_0)$  in (13),  $E[I_1 I_1^*](m_0)$  is derived as

$$E[I_1 I_1^*](m_0) = \sum_{m=0}^{M-1} P_1(m) \Gamma^{11}(m, m_0) + \sum_{m=0}^{M-1} P_2(m) \Gamma^{12}(m, m_0)$$

In practice, only  $L$  subcarriers are used ( $L < M/2$ ). Let us denote  $\mathcal{A}_{use}$  the set of used subcarriers,  $|\mathcal{A}_{use}| = L$ ;  $\mathbf{\Gamma}_1$ , (resp.  $\mathbf{\Gamma}_2$ ) the matrix that contains the coefficient  $\Gamma^{11}(m, m_0)$ , (resp.  $\Gamma^{12}(m, m_0)$ ),  $\forall m, m_0 \in \mathcal{A}_{use}$ ;  $\mathbf{P}_1 = [P_1(m)]$ ,  $\mathbf{P}_2 = [P_2(m)]$ ,  $\forall m \in \mathcal{A}_{use}$  and  $\mathbf{P} = [\mathbf{P}_1 \ \mathbf{P}_2]^T$ . Then  $E[I_1 I_1^*](m_0)$  can be written as

$$E[I_1 I_1^*](m_0) = [[\mathbf{\Gamma}_1 \ \mathbf{\Gamma}_2] \mathbf{P}](m_0) = [\mathbf{W}_1 \mathbf{P}](m_0) \quad (31)$$

Similarly, we can derive  $E[I_1 I_2^*](m_0) = [\mathbf{W}_2 \mathbf{P}](m_0)$  and  $E[I_2 I_2^*](m_0) = [\mathbf{W}_3 \mathbf{P}](m_0)$  where  $\mathbf{W}_2$  and  $\mathbf{W}_3$  can be calculated in the same way as  $\mathbf{W}_1$ . Obviously,  $E[I_a I_b^*](m_0)$  depends on the power allocation  $\mathbf{P}$ .

Finally, the covariance matrix  $\mathbf{X}_{IN}(m_0)$  can be written as

$$\mathbf{X}_{IN}(m_0) = \begin{bmatrix} [\mathbf{W}_1 \mathbf{P}](m_0) + \sigma_1^2(m_0) & [\mathbf{W}_2 \mathbf{P}](m_0) \\ [\mathbf{W}_2^* \mathbf{P}](m_0) & [\mathbf{W}_3 \mathbf{P}](m_0) + \sigma_2^2(m_0) \end{bmatrix}$$

If the equal power allocation  $P_1(m) = P_2(m) = P$ ,  $\forall m \in \mathcal{A}_{use}$  is applied, we simplify  $\mathbf{X}_{IN}(m_0)$  as

$$P \begin{bmatrix} \text{tr}(\mathbf{W}_1(m_0, :)) + \frac{\sigma_1^2(m_0)}{P} & \text{tr}(\mathbf{W}_2(m_0, :)) \\ \text{tr}(\mathbf{W}_2^*(m_0, :)) & \text{tr}(\mathbf{W}_3(m_0, :)) + \frac{\sigma_2^2(m_0)}{P} \end{bmatrix} \quad (32)$$

$$= P \mathbf{W}(m_0)$$

where  $\mathbf{W}_i(m_0, :)$  is the  $m_0$ -th row vector of matrix  $\mathbf{W}_i$  and  $\text{tr}(\mathbf{S})$  is the trace of vector  $\mathbf{S}$ . Note that if  $\frac{\sigma_i^2(m)}{P} \ll \text{tr}(\mathbf{W}_i(m_0, :))$ ,  $\mathbf{W}(m_0)$  can be assumed independent from  $P$ .

#### REFERENCES

- [1] L. Stadelmeier, D. Schneider, D. Schill, A. Schwager, and J. Speidel, "MIMO for inhome Power Line Communications," *International Conference on Source and Channel Coding (SCC)*, 2008.
- [2] R. Hashmat, P. Pagani, A. Zeddani, and T. Chonavel, "MIMO communications for inhome PLC networks: Measurements and results up to 100 MHz," *ISPLC*, 2010.
- [3] F. Versolatto and A. M. Tonello, "A MIMO PLC random channel generator and capacity analysis," *IEEE ISPLC 2011*, pp. 66–71, 2011.
- [4] B. Nikfar and A. J. H. Vinck, "Combining techniques performance analysis in spatially correlated MIMO-PLC systems," *IEEE ISPLC 2012*, pp. 1–6, 2012.
- [5] R. Hashmat, P. Pagani, A. Zeddani, and T. Chonavel, "A channel model for multiple input multiple output in-home power line networks," *ISPLC*, 2011.
- [6] A. M. Tonello, F. Versolatto, B. Béjar, and S. Zazo, "A fitting algorithm for random modeling the PLC channel," *IEEE Trans. Pow. Del.*, vol. 27(3), pp. 1477–1484, 2012.
- [7] Seventh Framework Programme: Theme 3 ICT-213311 OMEGA, Deliverable D3.2, "PLC Channel Characterization and Modelling," Information and Communication Technologies (ICT), Tech. Rep., 2011, v1.2.
- [8] M. Zimmermann and K. Dostert, "A multipath model for the powerline channel," *IEEE Trans. Commun.*, vol. 50(4), pp. 553–559, 2002.
- [9] A. M. Tonello, "Wideband impulse modulation and receiver algorithms for multiuser power line communications," *EURASIP Journal on Advances in Signal Processing*, pp. 1–14, 2007.
- [10] P. Achaichia, M. L. Bot, and P. Siohan, "OFDM/OQAM: A solution to efficiently increase the capacity of future PLC networks," *IEEE Trans. Pow. Del.*, vol. 26(4), pp. 2443–2455, 2011.
- [11] I. C. Society, *IEEE Standard for Broadband over Power Line Networks: Medium Access Control and Physical Layer Specification.*, 2010.
- [12] A. Cortés, J. Cañete, L. Díez, and M. Torres, "On PLC channel models: an OFDM-based comparison," *ISPLC*, 2013.
- [13] S. Krusevac, P. Rapajic, and R. A. Kennedy, "Channel capacity estimation for MIMO systems with correlated noise," *IEEE GLOBECOM*, pp. 2812–2816, 2005.
- [14] R. Hashmat, P. Pagani, and T. Chonavel, "Analysis and modeling of background noise for inhome MIMO-PLC channels," *ISPLC*, 2012.